Preparation of Cylindrical Multi-Compartment Micelles by the Hierarchical Self-Assembly of ABC Triblock Polymer in Solution

ARTICLE *in* RSC ADVANCES · SEPTEMBER 2015

Impact Factor: 3.84 · DOI: 10.1039/C5RA19002A

5 AUTHORS, INCLUDING:

Yi Shi

University of Notre Dame

21 PUBLICATIONS **230** CITATIONS

SEE PROFILE

RSC Advances

PAPER

View Article Online
View Journal | View Issue

Cite this: *RSC Adv.*, 2015, **5**, 85446

Preparation of cylindrical multi-compartment micelles by the hierarchical self-assembly of ABC triblock polymer in solution

Arzugul Muslim,[ac] Yi Shi,[b] Yechao Yan,[b] Dongdong Yao[b] and Abulikemu Abudu Rexit*[ac]

Received 15th September 2015
Accepted 22nd September 2015

DOI: 10.1039/c5ra19002a

www.rsc.org/advances

Amphiphilic linear ABC triblock copolymer P*n*BA$_{28}$-*b*-PS$_{37}$-*b*-P2VP$_{73}$ was prepared by the RAFT method and its two-step hierarchical self-assembly in selected solvents was explored. The triblock copolymer was refluxed in methanol and the micelle product was further dialyzed against acidic water. The effects of the concentration of copolymer on the morphology of the aggregates formed in methanol in the first step were investigated. The structures and morphologies of the micelles formed by the self-assembly were characterized with SEC, ^{1}H NMR, TEM and DLS. Spherical patchy micelles were obtained in the poor solvent, methanol, for PS and P*n*BA blocks during the first step assembly. The patchy micelles were dialyzed against water with a pH value of ~3.0 and aggregated to form multi-compartment micelles (MCMs). The MCMs further aggregated when the concentration of patchy micelles was increased. Cylindrical MCMs were formed with 2 mg mL^{-1} patchy micelles.

Introduction

Block copolymers can be self-assembled to form various controllable nanoscale ordered structures and morphologies,[1–3] which has attracted considerable attention in nanotechnology research field.[4] ABC triblock copolymers can be self-assembled in the appropriate selected solvent, according to the assembling conditions for each block, to form nanoscale aggregates with various structures and morphologies. In the selected solvent for one block where the other two blocks are insoluble, the insoluble two blocks form a micelle core. These two blocks can separate into two phases in a tens of nanometer space, resulting in multi-compartment micelles (MCMs).[1,5–10] Large number of micro-segments are formed in the cores and shells of MCMs, leading to a complex micellar morphology. MCMs incorporate different payloads in individual compartments and can be used to load particles with different chemical properties. Therefore, it is potentially useful in drug delivery and controllable release as well as the preparation of special nanostructured materials.[2]

Generally, MCMs are prepared by the self-assembly of diblock copolymer blends,[11,12] self-assembly of triblock copolymers with various topologies[2,13–32] and multiblock[33–35] copolymers in selective solvents, annealing of the self-assembled copolymer aggregates, changing the self-assembly behavior of the copolymers in the selected solvent by the fluorination of one block in the copolymers, self-assembly between copolymers and assembly between copolymer and small molecules. The most widely used method for the preparation of MCMs with ABC triblock copolymers is to select a good solvent for one block that is soluble to the solvent to form the corona of MCMs. The other insoluble two blocks form the core domain of compartmentalized core of the MCMs.[2,16,17,19–21,36–40] Müller *et al.* proposed a two-step hierarchical self-assembly approach for the preparation of MCMs.[2,17,18,22,36,41,42] Primary micelles, with one block as corona and the other blocks as compartmentalized core were prepared in the selected solvent for the corona block. Secondary aggregation of the micelles was then induced by dialysis to form multi-compartment micelles. This is a striking success in the preparation of MCMs with controllable aggregation between MCMs.[8]

The self-assembly behavior of ABC triblock copolymers in solution especially to form MCMs, is not well understood as that of diblock copolymers.[5] There is no efficient simple synthesis method for the preparation of MCMs with triblock copolymers. Strong phase separation ability is required for the triblock copolymers. Generally, fluorine-containing polymers are selected, which is a challenge for polymer synthesis and limits the performances and applications of resultant MCMs. The morphology of the triblock MCMs aggregates can be tuned

[a]*School of Chemistry and Chemical Engineering, Xinjiang Normal University, Urumqi, China. E-mail: aarexit@mail.ustc.edu.cn; Fax: +86 0991 4332683*

[b]*Laboratory of Polymer Physics and Chemistry, Institute of Chemistry, The Chinese Academy of Science, Beijing, China*

[c]*School of Chemistry and Material Science, North West University, Xi'an, China. E-mail: arzu_hma@yahoo.com*

by the optimizing assembly conditions, such as the block sequence, ratio of the composite blocks, composite of solvent, concentration of the copolymer, temperature, time and so on.[1,9,42,43] The initial concentration of the copolymer can affect the stretch of the compartmentalized core, the interfacial tension between the micellar core and solvent, interactions between coronas, and so on,[42] which further affects the self-assembly of the triblock copolymers in solution. In the present work, cylindrical MCMs were prepared from ABC triblock copolymer by tuning the concentration of the copolymer and solvents.

The micro-segments formed in compartmentalized core or shell are the prerequisite for the formation of the cylindrical MCMs. Thus, the structural design of the ABC triblock copolymer is critical. In the present work, triblock copolymer, P*n*BA-*b*-PS-*b*-P2VP, was designed due to the different solubility of the three blocks in methanol and acidic water and its easy synthesis. It is well known that P2VP is quaternized under pH stimuli and can form hydrogen bonds with metal salt complexes and phenolic hydroxyl groups. P*n*BA is in rubbery state at room temperature and has a strong interfacial tension with water. PS has a high glass transition temperature (T_g) of 100 °C and is in glassy state at room temperature. It can stabilize the morphology of the MCMs during the self-assembly process.[44] The properties of each block provide the multiple functions of the prepared MCMs and stabilize the MCMs solution. Linear triblock copolymer, P*n*BA$_{28}$-*b*-PS$_{37}$-*b*-P2VP$_{73}$, with narrow molecular weight range was successfully synthesized by the reversible addition–fragmentation chain transfer (RAFT) radical polymerization. The ABC triblock copolymer was refluxed in methanol. The P*n*BA and PS blocks formed the core with phase-separated domains of the resultant primary MCMs and soluble P2VP formed the shell of the micelles. The primary MCMs were dialyzed against acidic water to increase their phase separation ability. The high level cylindrical MCMs were obtained by adjusting the initial concentration of the triblock copolymer. The mechanism of this process is shown in Scheme 1.

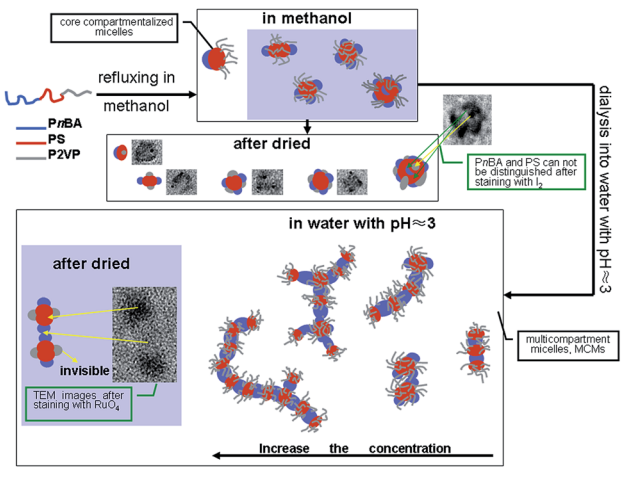

Scheme 1 Mechanism of hierarchical self-assembly process of P*n*BA$_{28}$-*b*-PS$_{37}$-*b*-P2VP$_{73}$ in solution.

Experimental

Materials and reagents

Azobisisobutyronitrile (AIBN) was recrystallized in ethanol. *N*-butyl acrylate (*n*BA), styrene (St) and 2-vinylpyridine (2VP) were purchased from Alfa Aesar (Ward Hill, MA), dehydrated on CaH_2 and distilled under reduced pressure. *N*,*N*-Dimethylformamide (DMF) was dried over anhydrous magnesium sulfate and distilled under reduced pressure. Other reagents were of analytical grade and used as received.

Instruments and methods

Size Exclusive Chromatography (SEC) measurements were performed on Styragel HT2, HT4 and HT5 gel columns at 50 °C. The analytes were eluted with DMF driven by Waters 515 HPLC pumps and at 1.0 mL min^{-1}. PS was used as a standard and the analytes were monitored with a Waters 2414 parallax refractive index detector. Nuclear magnetic resonance spectra (^{1}H-NMR) were recorded on a Bruker DMX400 spectrometer at room temperature with $CDCl_3$ as solvent and TMS as internal standard. Transmission electron microscopy (TEM) images were taken with on a TECNAI G^{2}20 TEM operated at an accelerating voltage of 200 kV. The machine was equipped with a digital camera. The micellar solution was dispersed on a copper lined pure carbon film and dried at room temperature. The primary patchy micelles were stained with I_2 and the secondary micellar products were stained with RuO_4. DLS measurements were performed at a scattering angle of 30° on an ALV DLS/SLS-SP 5022F equipment consisting of an ALV-SP 125 laser goniometer, an ALV 5000/E correlator and a He–Ne laser operating at a wavelength of $\lambda = 632.8$ nm. Test temperature was 25 °C and the test time was 1 h. Organic sample were filtered with 0.45 μm Millipore nylon filters and aqueous samples were filtered with 0.45 μm Millipore PVDF filters.

Synthesis of P*n*BA$_{28}$-*b*-PS$_{37}$-*b*-P2VP$_{73}$ copolymer

Synthesis of P*n*BA$_{28}$. The RAFT agent S-1-ethyl-S′-(α,α′-dimethyl-α-dimethyl-α″-acetic acid) trithiocarbonate (EDMAT) was prepared according to the previous report.[44] The initiator AIBN (2.54 mg), RAFT agents EDMAT (70 mg) and monomer *n*BA (8 g) were completely dissolved in 1.6 g acetone in a polymerization tube, frozen in liquid nitrogen, flushed with nitrogen, vacuumed and melted. This procedure was repeated 3 times. The reaction tube was sealed and heated at 60 °C for 4.5 h. The product was then diluted with tetrahydrofuran (THF) and precipitated in 200 mL methanol/water (v/v, 1 : 1). The supernatant was removed and the solvent residue was removed by rotary evaporation. The precipitation was repeated three times and the final product P*n*BA$_{28}$ was vacuum-dried at room temperature for 12 h.

Synthesis P*n*BA$_{28}$-*b*-PS$_{37}$ diblock copolymer. P*n*BA$_{28}$ containing terminal group of RAFT agent (0.35 g) was dissolved in 2.08 g St in a polymerization tube, frozen in liquid nitrogen, flushed with nitrogen, vacuumed and melted. The procedure was repeated three times. The reaction tube was sealed and heated at 90 °C for 3 h. The polymerization solution was diluted

with THF, precipitated in 200 mL methanol/water (v/v, 4 : 1) and leached. The precipitation was repeated three times and the final product P*n*BA$_{28}$-*b*-PS$_{37}$ was vacuum-dried at room temperature for 12 h.

Synthesis of P*n*BA$_{28}$-*b*-PS$_{37}$-*b*-P2VP$_{73}$ triblock copolymer. AIBN (0.17 mg), P*n*BA$_{28}$-*b*-PS$_{37}$ diblock copolymer (0.31 g), 2VP (0.84 g) were dissolved in 1.15 g 1,4-dioxane, frozen in liquid nitrogen, flushed with nitrogen, vacuumed and melted. This procedure was repeated three times. The reaction tube was sealed tube and heated at 60 °C for 8 h. The polymerization solution was diluted with THF and precipitated in petroleum ether. The supernatant was removed and the solvent residue was removed by rotary evaporation. The precipitation was repeated three times and the final product was vacuum-dried at room temperature for 12 h.

Self-assembly of MCMs. P*n*BA$_{28}$-*b*-PS$_{37}$-*b*-P2VP$_{73}$ triblock copolymer solution was subjected to a two-step hierarchical self-assembly procedure. Triblock copolymers with amounts of 2 mg, 5 mg, 10 mg, 20 mg and 40 mg, respectively, are refluxed in 20 mL methanol overnight and cooled to room temperature to obtain primary MCMs. Five milliliters MCMs solution was dialyzed against water with a pH value of ~3. The dialysis solution was changed every 3.5 hours for 12 times to produce the final MCMs product.

Results and discussion

Synthesis of triblock copolymer by RAFT method

P*n*BA$_{28}$, P*n*BA$_{28}$-*b*-PS$_{37}$ and P*n*BA$_{28}$-*b*-PS$_{37}$-*b*-P2VP$_{73}$ were synthesized by RAFT method as shown in Scheme 2. Their SEC chromatograms and ^{1}H-NMR spectra are shown in Fig. 1 and 2, respectively.

All P*n*BA$_{28}$, P*n*BA$_{28}$-*b*-PS$_{37}$ and P*n*BA$_{28}$-*b*-PS$_{37}$-*b*-P2VP$_{73}$ polymers showed a single symmetrical peak and the peaks of diblock and triblock copolymers shifted to higher molecular weight region, indicating that the copolymerization was effectively controlled. In addition, the molecular weight distributions of the resultant polymers are in a narrow range (PDI≤1.32) (Table 1), indicating the formation of the products in a narrow molecular range. The ^{1}H NMR spectra of P*n*BA-*b*-PS-*b*-P2VP indicate the desired product was produced. The degree of polymerization (DP) of P*n*BA was calculated with the

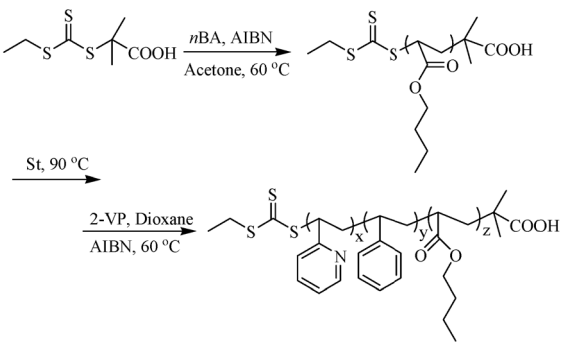

Scheme 2 Synthetic route of block copolymers.

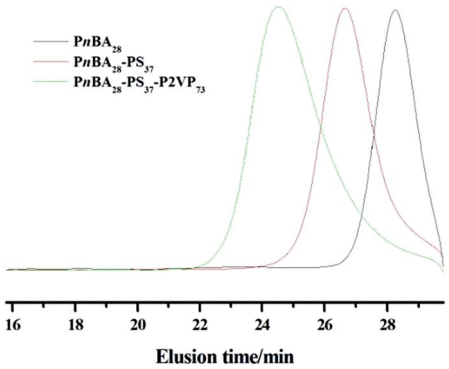

Fig. 1 SEC curves of block copolymers in DMF.

area ratio of the peak at δ = 2.3 ppm that was assigned to the hydrogen of the methine group in *n*BA repeating unit to the peak at δ = 3.8 ppm that was assigned to the hydrogen of methylene in EDMAT (Table 1). Similarly, the DPs of PS and P2VP were calculated with the area ratios of the hydrogen peak of methine in *n*BA repeating units at δ = 2.3 ppm to the hydrogen peak of benzene ring in PS units at δ = 6–7.2 ppm and to the hydrogen peak of –N=CH– of pyridine ring in P2VP units at δ = 7.8–8.6 ppm, respectively (Table 1). The polymer molecular weights obtained with SEC are the relative molecular weights to PS, and thus they are different from those obtained with ^{1}H NMR (Table 1).

Self-assembly behaviors of P*n*BA$_{28}$-*b*-PS$_{37}$-*b*-P2VP$_{73}$ solution

Linear triblock copolymer P*n*BA$_{28}$-*b*-PS$_{37}$-*b*-P2VP$_{73}$ was hierarchically self-assembled with a two-step procedure. At the primary step as shown in Fig. 3, P*n*BA$_{28}$-*b*-PS$_{37}$-*b*-P2VP$_{73}$ copolymer samples with amounts of 2 mg, 5 mg, 10 mg, 20 mg and 40 mg were, respectively, refluxed in 20 mL methanol at 80 °C overnight, cooled to room temperature and stained with I_2. The secondary micelle product was prepared by dialyzing the primary assembled micelles at the first step against the water with a pH value of ~3. Fig. 4 shows the TEM images of the dispersed secondary micellar particles stained with RuO_4. Fig. 5

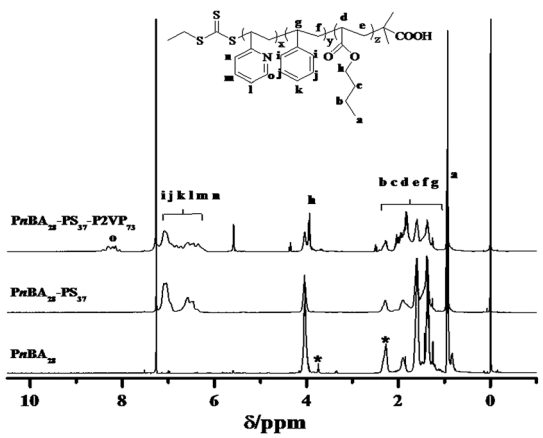

Fig. 2 ^{1}H NMR spectrum of block copolymers.

Table 1 Structural characterization data of block copolymers

Samples	$M_{H\ NMR}$[a]	M_n[b]	M_w[b]	M_w/M_n
P*n*BA$_{28}$	3580	18 100	19 400	1.07
P*n*BA$_{28}$-*b*-PS$_{37}$	7430	33 500	38 100	1.13
P*n*BA$_{28}$-*b*-PS$_{37}$-*b*-P2VP$_{73}$	15 000	69 200	91 300	1.32

[a] Calculated from the following formula: $128 \times 28 + 104 \times DP_{st} + 105 \times DP_{2VP}$. [b] Obtained from SEC test.

is the DLS curves for the micelles obtained before and after dialysis, the relative data are shown in Table 2.

The TEM images of the primary self-assembled products formed on this step show that they are uniform 27 ± 5 nm spherical micelles (Fig. 3). It is worth noting that 2–5 black spots with sizes of several nanometers were observed on each micellar particle, indicating the phase separation in the micelle particles. I_2 stains P2VP microphase that is visualized as the dark patchy area on the TEM image. PS and P*n*BA microphase cannot be visualized with I_2 staining and cannot be identified on the TEM images. Therefore, the gray round area in the TEM images is corresponding to the PS and P*n*BA blocks. Methanol is a good solvent for P2VP block and poor solvent for PS and P*n*BA blocks. The polarity of P*n*BA is slightly higher than PS. Therefore, PS block was tangled together to form the core of the micelle during the first-step assembly. P*n*BA block collapsed on the PS surface to form island-like microphases, which, in combination with PS core, formed the multi-compartmentalized core of MCMs. P2VP extended on the core surface to form the shell of

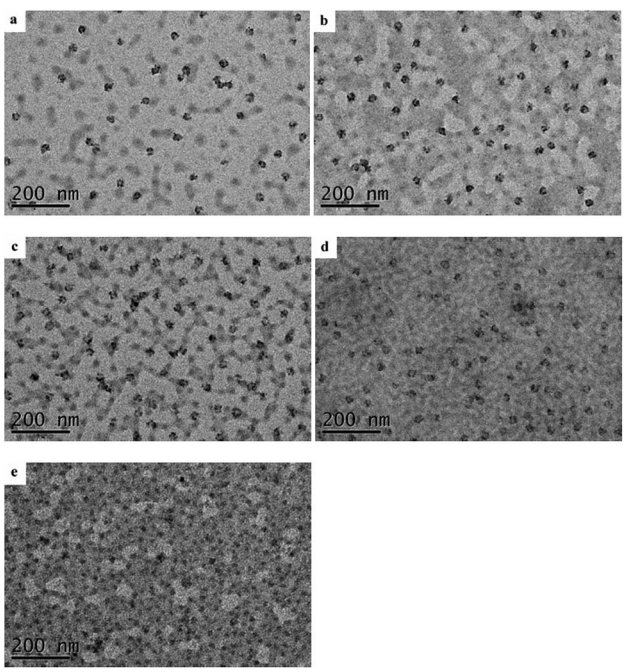

Fig. 3 TEM images of primary self-assembled micelles of P*n*BA$_{28}$-*b*-PS$_{37}$-*b*-P2VP$_{73}$. (a)–(e) were the self-assembled aggregates in different concentration in methanol: (a) 0.1 mg mL^{-1}, (b) 0.25 mg mL^{-1}, (c) 0.5 mg mL^{-1}, (d) 1.0 mg mL^{-1}, (e) 2.0 mg mL^{-1}, staining with I_2.

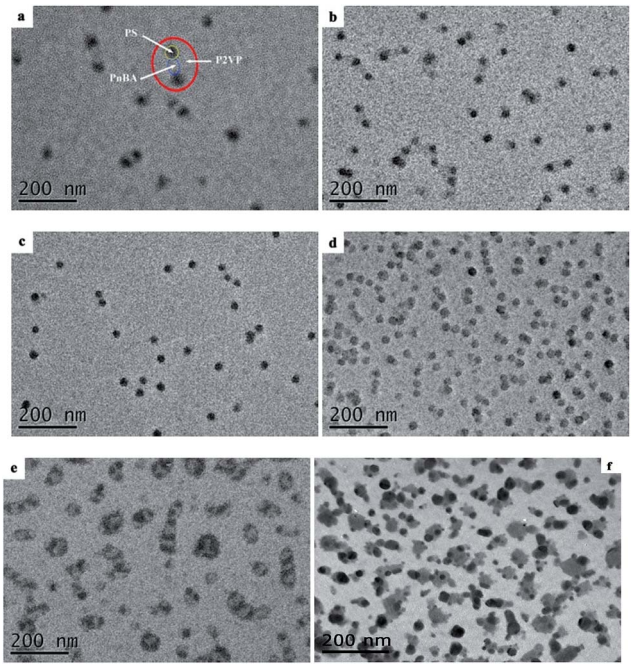

Fig. 4 TEM images of secondary self-assembled micelles of P*n*BA$_{28}$-*b*-PS$_{37}$-*b*-P2VP$_{73}$ prepared by dialyzing the primary assembled micelles at the first step against the water with a pH value of ~3, the first self-assembly concentration of samples were as following: (a) 0.1 mg mL^{-1}, (b) 0.25 mg mL^{-1}, (c) 0.5 mg mL^{-1}, (d) 1.0 mg mL^{-1}, (e) 2.0 mg mL^{-1}, staining with RuO_4. (f) is the image of (e) taken in 7 months later.

the micelle. In methanol that is the selected solvent for P2VP block, the microphases are in thermodynamic metastability due to their interactions with P2VP block.[44] Therefore, refluxing in methanol can activate the micelles and promote their self-assembly. P2VP block could also collapse on the PS surface due to solvent evaporation when the sample was dried for TEM imaging. Generally, the stained P2VP in the simple core–shell micelles exhibits anuniform continuous annular morphology. The island-like spots of the P2VP block in the MCMs prepared here indicate the phase separation between P2VP and P*n*BA, which leads to the morphologies as shown in Fig. 3a–e. Lodge *et al.*[37,38] demonstrated that the morphology of triblock copolymer micelle was decided by the competition between interface where the blocks with weak interactions tends to reach and the interface between covalent-bonded blocks. P2VP and P*n*BA are the blocks with weak interactions in their poor solvent methanol and P*n*BA/PS blocks and P2VP/PS blocks are covalent-bonded. P2VP block tends to expend on the surface of the micelle and P*n*BA block collapses on the core surface, leading to the formation patchy micelles. DLS results further confirm the assembly mechanism as described above and showed in Scheme 1. The assembled micelles from the block copolymer solutions with all concentrations except 0.25 mg mL^{-1} showed two narrow distribution peaks. Most particles have a radius of 20 nm (a diameter of 40 nm), which are patchy micelles. The number of the large micelles was increased with the increase of the concentration of block copolymers, indicating the possible aggregation between the patchy micelles. The scattered light of

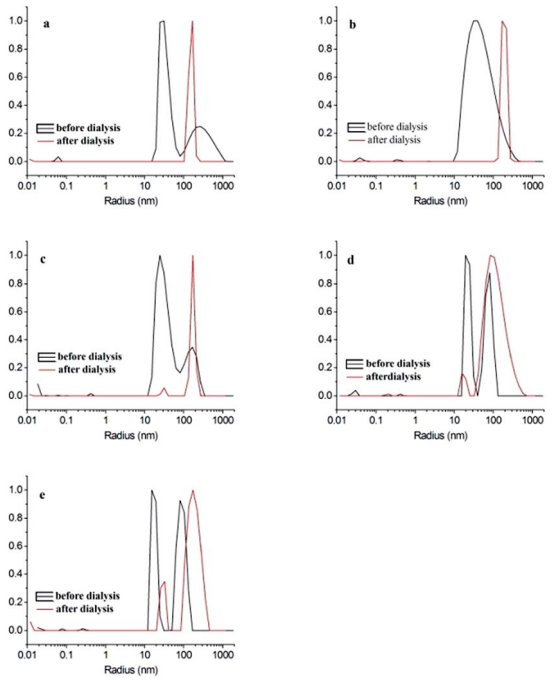

Fig. 5 DLS curves of P*n*BA$_{28}$-*b*-PS$_{37}$-*b*-P2VP$_{73}$ at different initial concentration: (a) 0.1 mg mL^{-1}, (b) 0.25 mg mL^{-1}, (c) 0.5 mg mL^{-1}, (d) 1.0 mg mL^{-1}, (e) 2.0 mg mL^{-1}.

large particles is stronger than that of smaller particle. The amount of particles with large sizes is actually very low even the intensity of its DLS peak is high.

As for the secondary micelle products shown in Fig. 4, RuO_4 stains PS block, which is appeared as the dark area on the TEM images of the secondary micelle products. Uniform spherical particles with a diameter of 41 ± 10 nm were observed in Fig. 4a–c. It is worth noting that gray lines were formed between these particles, indicating the possible formation of oligo-aggregates. According to the DLS images of the secondary micelle products, the R_h of these particles reached 150 nm (*i.e.*, 300 nm in diameter), which is much larger than the theoretical size of regular spherical micelles. These results indicate the formation of aggregate in the micellar solution. Further

Table 2 DLS data of P*n*BA$_{28}$-*b*-PS$_{37}$-*b*-P2VP$_{73}$

Concentration of samples	Self-assembly process	Radius (nm)
0.1 mg mL^{-1}	Before dialysis	67.9
	After dialysis	154.7
0.25 mg mL^{-1}	Before dialysis	46.3
	After dialysis	190
0.5 mg mL^{-1}	Before dialysis	44.9
	After dialysis	30.6
		172.5
1.0 mg mL^{-1}	Before dialysis	22.3
		75.4
	After dialysis	17.4
		111.4
2.0 mg mL^{-1}	Before dialysis	17.4

increase of the concentration of copolymers to 1 mg mL^{-1} led to short bead chain-like aggregates (Fig. 4d). The short 200 nm long cylindrical aggregates consisting of ~100 nm spherical particles were formed in the micelle solution prepared with 2 mg mL^{-1} triblock copolymers (Fig. 4e). Based on the structural feature and sizes of these aggregates, the particles with clear boundaries between black and gray regions are not formed in methanol during the first step of the self-assembly. The black area is the image of PS microphase and the gray particles are the P*n*BA phase, which form the cylindrical aggregated particles in an alternating order. The bigger spherical particles are also composed of black and gray areas. The acidic solution is a good solvent for P2VP. Thus, P2VP can extend on the surface of the phase separated PS-P*n*BA compartmentalized core during TEM imaging. PS is in a frozen state in methanol at room temperature due to its high T_g. The size reassembly of the block copolymer in the patchy micelles could not occur when the solvent was changed to high polar water. The P*n*BA microphases on the surfaces of different PS microphases can adhere together to form the secondary self-assembled aggregates(Scheme 1). Lodge *et al.*[38] prepared wormlike segmented MCMs by the self-assembly of star shaped ABC tri-block copolymer μ-EOF. Although they believed that the aggregation between MCMs could be achieved through sharing their micelle coronas, but they also demonstrated micelle coronas have steric repulsions between each other. Therefore, P2VP cannot stabilize the hydrophobic core due to the environmental change, leading to the secondary self-assembly. Meanwhile, the frozen PS microphase hinders the molecular level self-assembly to form a more stable structure, leading to the merging of P*n*BA patches to reduce the free energy. The relationship between the secondary self-assembly and the concentration of polymer concentration further confirms this hypothesis.

The shape diversity of the secondary micelles is related to the number of patches in the primary micelles. As shown in Fig. 3, most of primary micellar particles contain two patches, which form segmented cylindrical micelles during secondary self-assembly.

These also promote the aggregation of MCMs assembled from primary patchy micelles to lower the free energy of the system. Therefore, chain-like aggregates of the MCMs and patchy micelles were observed in the secondary assembled samples (Fig. 4a–e). The length of the aggregate chain was increased with the increase of the concentration of the triblock copolymer and complete segmented cylindrical MCMs with separated phases were obtained with 2.0 mg mL^{-1} P*n*BA$_{28}$-*b*-PS$_{37}$-*b*-P2VP$_{73}$ solution (Fig. 4e). The dark area on the TEM image of the MCMs is the PS microphase and the lighter area is the P*n*BA microphase. P2VP block cannot be visualized with the RuO_4 staining. The PS blocks (dark area in Fig. 4e) are segregated by the bigger P*n*BA blocks (light area in Fig. 4e) in the cylindrical MCMs. The high concentration and enhanced interfacial tension between P*n*BA and water leads the aggregation of patchy micelles through P*n*BA blocks, resulting in cylindrical MCMs (Scheme 1). Linear MCMs were formed through the adhesion between the micelles with two patches. Micelles with more than 2 patches functioned as the joint of the bifurcation in cylindrical MCMs. A

considerate amount of bifurcated cylindrical MCMs were first observed in MCMs formed with 2 mg mL^{-1} triblock copolymers (Fig. 4e). Zhu *et al.*[45] found that wormlike PS-*b*-P2VP-*b*-PEO self-assembled segmented MCMs remained stable under operations as strong mechanic stirring and ultrasonic vibrating. They believed that the micelle chains strongly interacted with each other, leading to the wormlike morphology. Fig. 4f shows the TEM image stained with RuO_4 of segmented cylindrical MCMs taken in 7 months later. As can be seen, the segmented cylindrical MCMs obtained in the present work were slightly broken. The number of cylindrical micelles was slightly decreased. However, the spherical micelles tend to form cylindrical micelles. Compared with the micelles in Fig. 4e, the compartmentalized cores which are at the middle part of MCMs significantly were swelled. This might be attributed to the evaporation of the water during the storage. Therefore, the broken morphology of segmented cylindrical MCMs can be attributed to the change in their interaction with the solvent. In addition, Lodge *et al.*[38] reported that μ-EOF self-assembled segmented wormlike MCMs were in thermodynamic metastability due to the slow or inhibited chain exchange between spherical MCMs. The results obtained in the present work may also be caused by the similar reasons.

The DLS analysis shows that the average radius of the secondary assembled MCMs is longer than that of the primary assembled MCMs, indicating severe P*n*BA collapse on the core surface, bigger multi-compartmentalized core and the accelerated aggregation between MCMs during the secondary self-assembly (Fig. 5). The size distribution of secondary MCMs, prepared with copolymer solutions with concentrations $\leq$0.5 mg mL^{-1}, is narrow and the intensities of their peaks are identical, indicating the MCMs or the high level aggregates are similar under these conditions (Fig. 5a–d). The MCMs became bigger when the concentration of the copolymer was increased to 2.0 mg mL^{-1}, indicating the formation of large amount of patchy micelles or the involvement of MCMs in higher level aggregation (Fig. 5e). P2VP shell swells during dialysis, which segregates the patchy micelles or MCMs prepared with low concentration copolymer solutions during the dialysis. More patchy micelles or MCMs are formed with high concentration of copolymers and they are closer or even contact directly with each other, leading to "effective collision" and aggregation between the insoluble core blocks to decrease the interfacial tension.[41] Generally, the size distribution of the MCMs formed by the dialysis of the micelle with concentrations lower than its critical aggregation concentration (CAC) is narrow. In contrast, the dialysis of the micelle with concentration higher than its CAC or containing more primary aggregated micelles leads to "effective collision". Thus, the CAC of the secondary assembly is slightly lower than 1.0 mg mL^{-1}.

Conclusions

In the present work, P*n*BA_{28}-*b*-PS_{37}-*b*-$P2VP_{73}$ triblock copolymer was prepared and its two-step hierarchical self-assembly was investigated. The effects of the concentration of copolymer used during the primary self-assembly on the morphology of MCMs were explored. Patchy micelles with PS and P*n*BA as multi-compartmentalized core and P2VP as shell were obtained in the poor solvent for PS and P*n*BA during the primary self-assembly process. The secondary self-assembly was conducted by dialyzing the patchy micellar solutions with various concentrations against the water with pH value of ~3.0 to form MCMs. When the concentration was increased to 2 mg mL^{-1}, the concentration of P*n*BA_{28}-*b*-PS_{37}-*b*-$P2VP_{73}$ in the dialysis solution is higher than its CAC. "Effective collision" occurred between the aggregated patchy micelles and MCMs or between the closely contacted patchy micelles and MCMs, resulting in cylindrical MCMs with separated phases. In full, cylindrical MCMs with multi-phase can be obtained simply by tuning selective solvent and the concentration of the copolymer.

Acknowledgements

Financial support by National Science Foundation of China for Youth Scholars (21104063) is greatly acknowledged.

Notes and references

1 W. Ian and G. J. Liu, *Polymer*, 2013, **54**, 1950.
2 F. Schacher, A. Walther and A. H. E. Müller, *Langmuir*, 2009, **25**, 10962.
3 J. W. Hu, G. J. Liu and G. Nijkang, *J. Am. Chem. Soc.*, 2008, **130**, 3236.
4 C. M. Park, J. S. Yoon and E. L. Thomas, *Polymer*, 2003, **44**, 6725.
5 N. Hadjichristidis, H. Iatrou, M. Pitsikalis, S. Pispas and A. A. Vgeropoulos, *Prog. Polym. Sci.*, 2005, **30**, 725.
6 H. J. Dou, G. J. Liu, J. Dupont and L. Z. Hong, *Soft Matter*, 2010, **6**, 4214.
7 C. A. Fustin, V. Abetz and J. F. Gohy, *Eur. Phys. J. E*, 2005, **16**, 291.
8 A. O. Moughton, M. A. Hillmyer and T. P. Lodge, *Macromolecules*, 2012, **45**, 2.
9 T. Jiang, L. Q. Wang, S. L. Lin, J. P. Lin and Y. L. Li, *Langmuir*, 2011, **27**, 6440.
10 A. Hanisch, A. H. Gröschel, M. Förtsch, D. Markus, J. Hiroshi, T. M. Ruhland, F. H. Schache and A. H. E. Müller, *ACS Nano*, 2013, **7**, 4030.
11 J. T. Zhu and R. C. Hayward, *Macromolecules*, 2008, **41**, 7794.
12 E. W. Price, Y. Y. Guo, C. W. Wang and M. G. Moffitt, *Langmuir*, 2009, **25**, 6398.
13 G. Yu and A. Eisenberg, *Macromolecules*, 1998, **31**, 5546.
14 J. F. Gohy, N. Willet, S. Varshney, J. X. Zhang and R. Jérôme, *Angew. Chem., Int. Ed.*, 2001, **40**, 3214.
15 X. Z. Jiang, G. Y. Zhang, N. Ravin and S. Y. Liu, *Langmuir*, 2009, **25**, 2046.
16 K. Skrabania, A. Laschewsky, H. Berlepsch and C. Böttcher, *Langmuir*, 2009, **25**, 7594.
17 F. Schacher, A. Walther, M. Ruppel, M. Drechsler and A. H. E. Müller, *Macromolecules*, 2009, **42**, 3540.
18 A. Wolf, A. Walther and A. H. E. Mülle, *Macromolecules*, 2011, **44**, 9221.

19 S. Kubowicz, J. F. Baussard, J. F. Lutz, A. F. Thünemann, H. Berlepsch and A. Laschewsky, *Angew. Chem., Int. Ed.*, 2005, **44**, 5262.
20 H. Berlepsch, C. Böttcher, K. Skrabania and A. Laschewsky, *Chem. Commun.*, 2009, **17**, 2290.
21 K. Skrabania, H. Berlepsch, C. Böttcher and A. Laschewsky, *Macromolecules*, 2010, **43**, 271.
22 A. Walther, C. Barner-Kowollik and A. H. E. Müller, *Langmuir*, 2010, **26**, 12237.
23 Z. Y. Chen, H. G. Cui, K. Hales, Z. B. Li, K. Qi, D. J. Pochan and K. L. Wooley, *J. Am. Chem. Soc.*, 2005, **127**, 8592.
24 Z. B. Li, Z. Y. Chen, H. G. Cui, K. Hales, K. Qi, K. L. Wooley and D. J. Pochan, *Langmuir*, 2005, **21**, 7533.
25 H. G. Cui, Z. Y. Chen, K. L. Wooley and D. J. Pochan, *Macromolecules*, 2006, **39**, 6599.
26 M. Uchman, M. Štěpánek and K. Procházka, *Macromolecules*, 2009, **42**, 5605.
27 B. Fang, A. Walther, A. Wolf, Y. Y. Xu, J. Y. Yuan and A. H. E. Müller, *Angew. Chem., Int. Ed.*, 2009, **48**, 2877.
28 A. Kotzev, A. Laschewsky and R. H. Rakotoaly, *Macromol. Chem. Phys.*, 2001, **202**, 3257.
29 S. Ritzenthaler, F. Court, L. David, E. Girard-Reydet, L. Leibler and J. P. Pascault, *Macromolecules*, 2002, **35**, 6245.
30 S. Ritzenthaler, F. Court, L. David, L. Leibler and J. P. Pascault, *Macromolecules*, 2003, **36**, 118.
31 Z. W. Ma, H. Z. Yu and W. Jiang, *J. Phys. Chem.*, 2009, **113**, 3333.
32 J. F. Gohy, E. Khousakoun, N. Willet, S. K. Varshney and R. Jérôme, *Macromol. Rapid Commun.*, 2004, **25**, 1536.
33 A. K. Brannan and F. S. Bates, *Macromolecules*, 2004, **37**, 8816.
34 A. F. Thünemann, S. Kubowicz, H. Berlepsch and H. Möhwald, *Langmuir*, 2006, **22**, 2506.
35 R. Hoogenboom, F. Wiesbrock, M. A. M. Leenen, H. M. L. Thijs, H. Huang, C. Fustin, P. Guillet, J. F. Gohy and U. S. Schubert, *Macromolecules*, 2007, **40**, 2837.
36 J. F. Lutz and A. Laschewsky, *Macromol. Chem. Phys.*, 2001, **206**, 813.
37 Z. B. Li, M. A. Hillmyer and T. P. Lodge, *Macromolecules*, 2006, **39**, 765.
38 Z. B. Li, E. Kesselman, Y. Talmon, M. A. Hillmyer and T. P. Lodge, *Science*, 2004, **306**, 98.
39 S. Zhong, H. G. Cui, Z. Y. Chen, K. L. Wooley and D. J. Pochan, *Soft Matter*, 2008, **4**, 90.
40 Z. L. Zhou, Z. B. Li, Y. Ren, M. A. Hillmyer and T. P. Lodge, *J. Am. Chem. Soc.*, 2003, **125**, 10182.
41 F. Schacher, E. Betthausen, A. Walther, H. Schmalz, D. V. Pergushov and A. H. E. Müller, *ACS Nano*, 2009, **3**, 2095.
42 A. H. Gröschel, F. H. Schacher, H. Schmalz, O. V. Borisov, E. B. Zhulina, A. Walther and A. H. E. Müller, *Nat. Commun.*, 2012, **3**, 710.
43 A. J. Convertine, B. S. Lokitz, Y. Vasileva, L. J. Myrick, C. W. Scales, A. B. Loweand and C. L. McCormick, *Macromolecules*, 2006, **39**, 1724.
44 J. L. Qin, Y. M. Chen, D. D. Yan and F. Xi, *Macromolecules*, 2010, **43**, 10652.
45 J. T. Zhu and W. Jiang, *Macromolecules*, 2005, **38**, 9315.

